Food Materials Research

ARTICLE

Open Access

https://doi.org/10.48130/fmr-0023-0035
Food Materials Research **2023**, 3:35

Preparation, structure and antimicrobial properties of modified gelatin composite hydrogel from chicken, bovine and porcine lung

Ye Zou[1,2,3], Xiaowen Wang[2,3], Liang Li[1,2,3], Lingjuan Wang[2,3], Yibo Lan[2,3], Xiaojuan Qin[3,4], Zhongjiang Wang[5], Daoying Wang[1,2,3*] and Weimin Xu[1,2,3*]

[1] *Jiangsu Key Laboratory for Food Quality and Safety-State Key Laboratory Cultivation Base, Ministry of Science and Technology, Nanjing 210014, PR China*
[2] *School of Food and Biological Engineering, Jiangsu University, 301 Xuefu Rd., Zhenjiang 212013, Jiangsu, PR China*
[3] *Institute of Agricultural Products Processing, Jiangsu Academy of Agricultural Sciences, Nanjing 210014, PR China*
[4] *Nanjing Qinrun Biotechnology Co., Ltd, Nanjing 210014, PR China*
[5] *College of Food Science, Northeast Agricultural University, Harbin 150030, Heilongjiang , PR China*
* Corresponding author, E-mail: wzjname@126.com; xuweimin@jaac.cn

Abstract

In this paper, the reaction process parameters of the hydrogel produced by the modified gelatin from chicken, bovine and porcine lungs with carboxymethyl chitosan (CMCS) and oxidized glucomannan (OKGM) were optimized to produce Schiff base reaction. The results showed the properties of the three composite hydrogels are improved when the value of gelatin/CMCS/OKGM reached 1:2:2. The best modified gelatin/CMCS/OKGM of bovine lung composite hydrogel (COBH) had a gelatin strength of 8.14 N, a swelling rate of 257%, a water evaporation rate of 66.86%, and an antibacterial property of 38.02%. The properties of modified gelatin/CMCS/OKGM of chicken lung composite hydrogel (COCH) were similar to those of COBH. However, the water holding capacity of COCH was higher than that of COBH. The properties of the modified gelatin/CMCS/OKGM for porcine lung composite hydrogel (COPH) were significantly decreased over those of the other two. Therefore, COCH has potential applications in food coating and preservation.

Citation: Zou Y, Wang X, Li L, Wang L, Lan Y, et al. 2023. Preparation, structure and antimicrobial properties of modified gelatin composite hydrogel from chicken, bovine and porcine lung. *Food Materials Research* 3:35 https://doi.org/10.48130/fmr-0023-0035

Introduction

In recent years, hydrogels, as an important new class of biomaterials, can be used by oxygen, drug molecules and other water-soluble small molecules through. Therefore, it is widely used in the fields of tissue engineering[1], drug delivery[2], edible films[3] and biosorbents[4]. Gelatin is homologous with collagen, it has good thermal reversibility, water binding ability, film forming, foaming and emulsifying ability. Gelatin can be converted to hydrogel by using physical, chemical and enzymatic treatments[5]. The search for alternative sources of bovine and porcine gelatin has been put on the agenda due to bovine spongiform encephalopathy and Islamic religious beliefs. Aquatic products also contain abundant collagen, but their thermal stability is worse than that of terrestrial organisms. Chicken lung contains a large amount of collagen, with a content of 3.0%−3.5%, which can be used for the extraction of gelatin. The annual slaughter volume of broilers is as high as 100 billion in China. Chicken lungs, as by-products of their processing, were mostly treated as waste. They were not only polluted the environment but also wasted resources. Through preliminary study by our team, it was found that chicken lungs were rich in collagen.

Carboxymethyl chitosan (CMCS), as a chitosan derivative, has physical and biological properties such as gelling, film-forming, antibacterial and good biocompatibility[6]. Cao et al.[7] prepared a CMCS/oxidized carboxymethylcellulose/curcumin film using the cast film method, which showed good color protection and mold growth inhibition for freshness preservation as a coated antibacterial material. Polysaccharide hydrogels have many advantages, but also disadvantages such as poor mechanical properties and unstable gelatin performance have limited their practical application in industrial production.

Konjac glucomannan (KGM) has good biocompatibility, high viscosity and is biodegradable[8] as well as regulating intestinal function, lipid metabolism[9] and other functions. During the oxidation reaction, aldehyde groups are generated in the KGM molecular chains, which are chemically cross-linked by the Schiff base reaction between the free amino group of CMCS and the aldehyde group of OKGM, enhancing the mechanical properties and functionality of the hydrogel[6]. In this paper, hybrid hydrogels were made by cross-linking lung-modified gelatin with CMCS and OKGM, and the structure and properties of the hydrogel composite system were analyzed. The effect of different OKGM mixing ratio on hydrogel performance was studied to find composite hydrogels with good performance.

Materials and methods

Materials and reagents

Modified gelatin of chicken, bovine and porcine lung was homemade in the laboratory, whose content of collagen was

20% and 30%, respectively. Briefly, lung gelatin is dissolved in phosphate solution followed by the addition of ethylenediamine and 1-Ethyl-3-(3-dimethylaminopropyl) carbodimide hydrochloride (EDC). The modified lung gelatin was obtained after heating at 37 °C for 2 h and filtering through a 3,500 kDa dialysis bag for 3 d. Carboxymethyl chitosan, konjac glucomannan, sodium periodate, and ethylene glycol were purchased from Shanghai Maclean Biochemical Technology Co., Ltd. (Shanghai, China). Brain heart infusion broth ulture medium was purchased from Qingdao Haibo Biotechnology Co., Ltd. (Qingdao, China). The remaining substances were all analytical-grade compounds and solvents.

Preparation of OKGM

The experimental method of OKGM preparation was using the method of Jiang et al.[10] with slight modification. KGM (5 g) was put into a 250 mL beaker. Deionized water (150 mL) was added and they were mixed well. They were divided into seven groups and 10 mL of 0.04, 0.06, 0.08, 0.10, 0.12, 0.14, and 0.16 g/mL of $NaIO_4$ solution was added dropwise, respectively. After measuring the optimal oxidant concentration conditions, the mixture was stirred in the dark, at room temperature for 8, 9, 10, 11, 12, 13, and 14 h, respectively. An equimolar amount of ethylene glycol with $NaIO_4$ was added and stirred for 2 h to terminate the reaction. The mixture was dialyzed with 3,500 kDa dialysis bag for 3 d until the solution was free of periodate (checked with silver nitrate). The dialysates were frozen and lyophilized in a freeze-dryer for subsequent measurements.

Determination of aldehyde group content in OKGM

The determination of aldehyde group content for OKGM was carried out according to the method of Yan et al.[11] with slight modification. OKGM (0.2 g) was dissolved in 50 mL of hydroxylamine-methyl orange hydrochloride solution and mixed well for 2 h. The samples were titrated with 0.1 mol/L NaOH standard solution and stopped when the color of the solution was changed from orange-red to light yellow with the last pH of 5.0. The titration curve was plotted using the volume of NaOH standard liquid consumed as the horizontal coordinate and the pH value as the vertical coordinate.

$$\text{Aldehyde group concentration} = \frac{\Delta V \times 0.001 \times n_{NaOH}}{W}$$

Where: ΔVis the volume of NaOH standard liquid consumed at the end of the titration. n_{NaOH} is the molar concentration of NaOH standard solution. W is the mass of OKGM.

Preparation of chicken, bovine and porcine gelatin/CMCS/OKGM composite hydrogels

In this experiment, CMCS (4%, w/v), OKGM (4%, w/v) and modified lung gelatin (15%, w/v) were used to prepare hydrogel by our previous study. The volume ratio of CMCS: aminized lung gelatin: OKGM solution was homogeneously mixed of 1:2:1, 1:2:2, 1:2:3, 1:2:4. Three of the above different mixture of chicken, bovine and porcine lung modified gelatin/CMCS/OKGM composite hydrogels, named COCH-1, COCH-2, COCH-3, COCH-4, COBH-1, COBH-2, COBH-3, COBH-4, COPH-1, COPH-2, COPH-3, and COPH-4, respectively, were prepared.

Infrared spectral analysis

FTIR spectroscopy was determined using the method described by Shi et al.[12]. The FTIR spectra of samples were analyzed with a 32 scans/min at a resolution of 4 cm^{-1} in 400 cm^{-1} and 4,000 cm^{-1}.

Scanning electron microscope characterization

The determination of scanning electron microscope (SEM) characterization was carried out as using the method of Shi et al.[12] with slight modification. The microstructure of the upper surface of the samples was visualized using a scanning electron microscope at an accelerating voltage of 10 kV. Prior to visualize, the samples were mounted on a brass stub and sputtered with gold in order to make the sample conductive, and photographs were taken at 8000× magnification for surface.

Determination of gelatin strength

Gelatin strength was determined using the method described by Fan et al.[13]. The texture instrument was set to TPA gel strength mode. The Bloom gel strength was determined with the texture analyser, which was set to a P36R probe with a starting force of 0.15 N and a speed of 2 mm/s to 80% deformation.

Determination of swelling rate

The experimental method of swelling rate of samples was carried out using the methods of Fan et al.[14] with slight modification. The hydrogels were freeze-dried into uniformly sized discs and the weight was recorded as M_0. The hydrogel was dissolved in PBS buffer of pH 7.4 at 37 °C, which was weighed again after every interval and recorded as M_1.

$$\text{Swelling rate ESR (\%)} = \frac{m_1 - m_0}{m_0} \times 100\%$$

Thermal variation analysis

The experimental method of thermal variation analysis was carried out using the methods of Bai et al.[4] with slight modification. The sample was placed in a thermogravimetric analyzer for thermal stability analysis. Dried samples (0.2 g) were scanned using a thermogravimetric analyser from 20 to 400 °C at a rate of 10 °C/min. Nitrogen was used as the purge gas at a flow rate of 60 mL/min.

Determination of moisture evaporation rate

The method of Liu et al.[15] was used to determinate moisture evaporation rate of the samples. The hydrogel was freeze-dried into uniform-sized discs. The hydrogel was immersed in distilled water and then left until it reached dissolution equilibrium. The water on the surface of the hydrogel was wiped away by absorbent paper and the weight was recorded as m_1. The hydrogel was then placed in a constant temperature oven and weighed periodically until constant.

$$\text{Moisture evaporation rate} = \frac{m_1 - m_2}{m_1 - m_3} \times 100\%$$

where m_1, m_2, m_3 are the initial weight, measured weight and final weight of the hydrogel, respectively.

Low field-nuclear magnetic resonance (LF-NMR) characterization

LF-NMR was calculated following the procedure outlined by Jiang[16]. An instrument was used to obtain relaxation

curves of the hydrogel at 25.0 °C. Sixteen scans (acquisitions) were accumulated to increase the signal-to-noise ratio. The recycle delay between the scans was 10 s to allow full spin relaxation. The pulse spacing was set to 0.4 ms between 90° and 180° pulses and the number of echoes was 15,000. Each sample was measured twice.

Antimicrobial properties

The method of Bian et al.[17] was used to measure antimicrobial properties of samples. The inhibition of COCH, COBH and COPH hydrogels on Staphylococcus aureus (*S. aureus*) and Escherichia coli (*E. coli*) was determined by spectrophotometry. The pH of the brain heart infusion medium was adjusted to 7.2 with NaOH solution, and then sterilized in an autoclave for 15 min. The prepared hydrogels were irradiated by UV for 1 h before the experiment, and the medium without hydrogels was used as a blank control. Three equal weights of hydrogels were added to the medium and mixed well and then 200 μL of diluted bacterial solution was inoculated into the medium. The absorbance values were measured at 600 nm after the samples were continuously oscillated at 37 °C and 120 r/min for 12 h.

$$\text{Bacteria inhibition rate} = \frac{A_0 - A_1}{A_0} \times 100\%$$

Where, A_1 is the absorbance after adding these composite hydrogels, and A_0 is the absorbance of the control group.

Statistical analysis

Means ± standard deviations were used to represent the data. SPSS 19.0 program, a one-way analysis of variance (ANOVA) and Duncan's test were performed to evaluate the differences between the data.

Results and discussion

Aldehyde group content of OKGM

The principle of oxidative modification for OKGM is to use oxidants to oxidize the hydroxyl groups on polysaccharides into carboxyl and aldehyde groups. The effect of aldehyde group content in OKGM after oxidation was explored by different oxidation times when oxidation temperature and $NaIO_4$ concentration were constant. As shown in Fig. 1a, the content of aldehyde group of OKGM was increased with the increase of oxidation time before 12 h. A maximum value of 7.96 mmol/g of aldehyde group content was occurred at 12 h of oxidation, which was used to oxidize OKGM.

The effect of different $NaIO_4$ concentrations on the content of aldehyde groups was investigated in oxidized OKGM at constant oxidation temperature and time. The results are shown in Fig. 1b. The aldehyde content in OKGM was gradually increased with the increase of $NaIO_4$ concentration. Due to the increase of $NaIO_4$ concentration, the cleavage of C=C of KGM into aldehyde groups was intensified, and the content of aldehyde groups was significantly increased. When the concentration of $NaIO_4$ was higher than 0.12 g/mL, the aldehyde content of OKGM was decreased with the increase of oxidant concentration. It was due to that, the aldehyde group on the chain of OKGM molecule might be combined with the unoxidized residual hydroxyl group to form a hemiacetal structure with the increase of $NaIO_4$ concentration. Therefore, the oxidation condition of OKGM was obtained by 0.12 g/mL $NaIO_4$ for 12 h to prepare hydrogel.

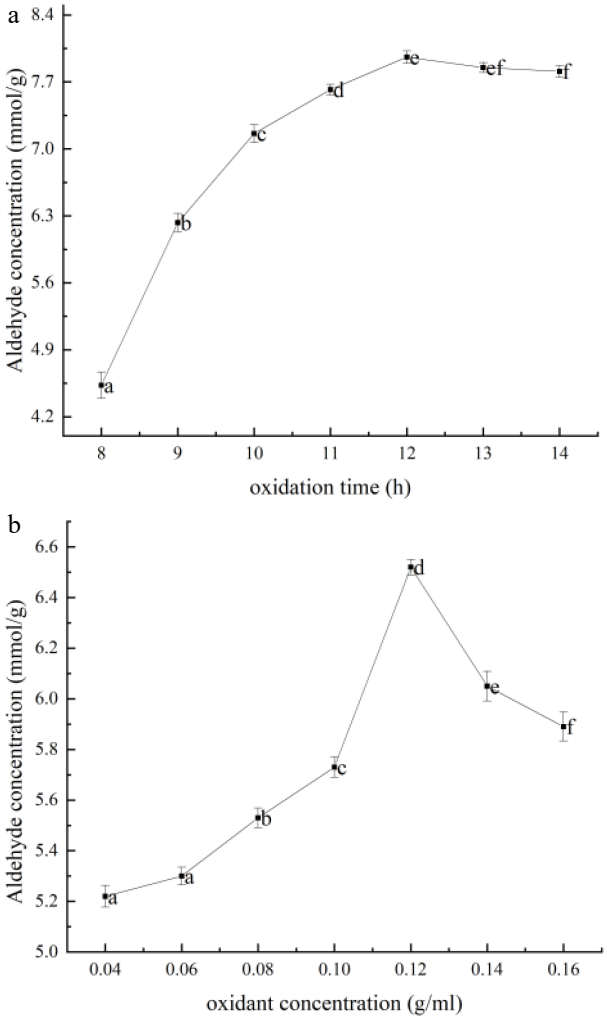

Fig. 1 Aldehyde content of OKGM prepared under different (a) oxidation times and (b) oxidant concentrations. The data in this figure is expressed as mean ± SD, different letters in this curve indicate significant differences ($p < 0.05$).

Infrared spectrogram

The infrared spectra of COCH, COBH and COPH in the range of 4,000–500 cm^{-1} are shown in Fig. 2. It can be seen that the three composite hydrogels COCH-1, COBH-1 and COPH-1 had the absorption peaks at 3,400, 1,638, 1,576, and 1,236 cm^{-1}. The wave number of 3,400 cm^{-1}, which were corresponded to the stretching vibrations of -OH and $-NH_2$. The absorption amide I band was corresponded to 1,638 cm^{-1}. The bending vibration peak of $-NH_2$ was at 1,576 cm^{-1}. The absorption peak of the symmetric stretching vibration of -COO- was at 1,416 cm^{-1}, and the absorption band of –OH was at 1,236 cm^{-1}[18].

When the ratio of OKGM increased, the spectrogram of COCH-2, COCH-3, COCH-4, COBH-2, COBH-3, COBH-4, COPH-2, COPH-3, and COPH-4 produced new vibrational stretching peaks of C=N bonds (1,638 cm^{-1}). This appearance indicated that the aldehyde group in the OKGM molecule was cross-linked with the amino group in the CMCS or lung gelatin

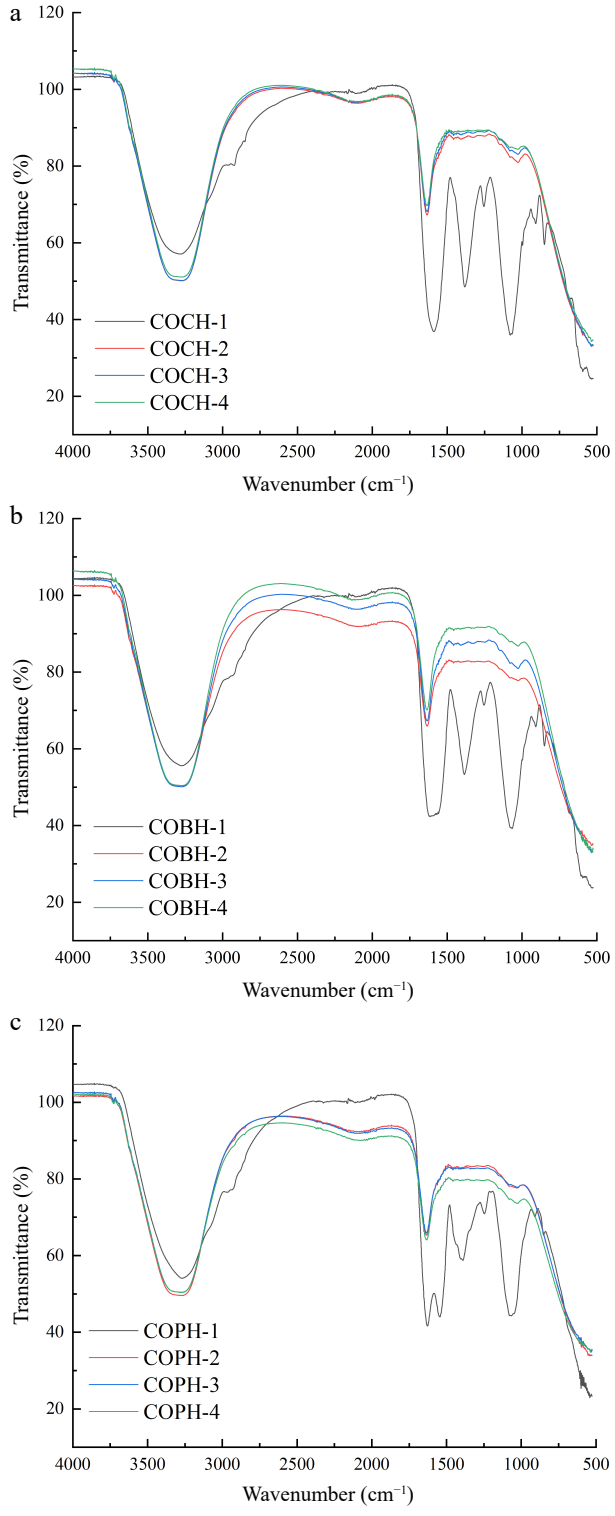

Fig. 2 Infrared spectra of (a) COCH, (b) COBH and (c) COPH with different mixing ratios.

molecule to form a composite hydrogel. This phenomenon was also found in the infrared spectra of carboxybutyryl chitosan-serine peptide/OKGM injectable hydrogels by Wang et al.[19] Additionally, when the proportion of OKGM was increased, the corresponding absorption peaks at 1,576 cm^{-1} and 1,236 cm^{-1} were weakened. It showed that the aldehyde group and the amino group had been condensed. The Schiff base reaction had been occurred, and the composite hydrogel had been successfully cross-linked. The broad absorption band of the three composite hydrogels at 3,300 cm^{-1} was the absorption peak of the stretching vibration of the O-H group and the N-H group. The absorption peak was become wider when the increase of the proportion of OKGM addition. It was possible that the -OH in KGM was interacted with the $-NH_2$ in CMCS to form a hydrogen bond. Therefore, a broader absorption peak appeared[20]. This phenomenon was consistent with the result of composite packaging films prepared by Tian et al.[21] The results showed that the three preparations had good compatibility and can be used as active ingredients to improve the composite hydrogels.

SEM

The role of porosity and interconnectivity in hydrogels is important for resistance to bacterial proliferation and water retention functions[22]. Figure 3 shows the internal microscopic morphology of various hydrogels at 20 μm. It was clear that all the composite hydrogels prepared by adding different proportions of OKGM had similar porous structures. The pores inside the hydrogel were interconnected and varied in size from 5–150 μm. The pore size of the composite hydrogel with a high percentage of OKGM was smaller than that of the composite hydrogel with a low percentage of OKGM. It was caused by the cross-linking between OKGM and CMCS, and the two had good compatibility and miscibility[23]. The crosslinking degree of the hydrogel was increased, the pore size was gradually reduced, and the pores were dense. More three-dimensional network structures were formed in the composite hydrogel. Similar conclusions were also obtained by Wu et al.[24]. When the OKGM ratio was increased, there were entangled clusters in SEM. It may be that the molecular weight of OKGM was large and some unreacted OKGM molecular chains were folded and bound to form tangled clusters. According to the microstructure, the porous internal structure within the composite hydrogel could be applied to drug encapsulation and slow release as well as cell culture utilization, etc.

Gelatin strength

The mechanical properties of COCH, COBH, and COPH are depicted in Fig. 4. As shown in Fig. 4, among the four hydrogels with the same configuration ratio, COBH had the highest gelatin strength, followed by COCH. However, COPH hydrogel had the lowest gelatin strength. According to the ratio of OKGM addition, the highest gelatin strength of hydrogel was obtained when the ratio of OKGM addition was 1:2:2. The lowest gelatin strength of hydrogel was obtained by the ratio of 1:2:4. The gelatin strength of the composite hydrogels in COCH, COBH, and COPH with a mixing ratio of 1:2:2 was significantly increased. The gelatin strength of the gelatin-chitosan-sodium alginate composite gelatin was 5.95 N as reported by Liu et al.[25]. The gelatin strength of the hydrogel made in this study was increased four times, compared with the chitosan/bletin gum hydrogel (202.40 ± 6.35 g) prepared by Luo et al.[26]. These results indicated that the gelatin strength of the hydrogels was increased to some extent with the increase of OKGM content, which showed a positive

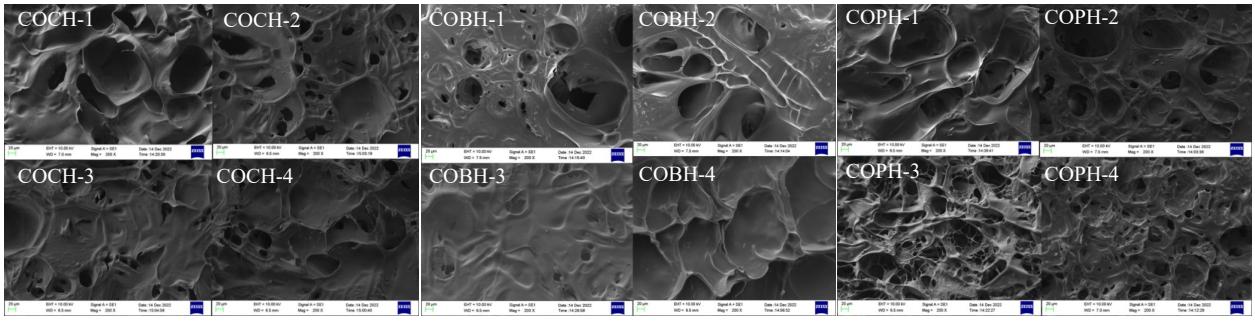

Fig. 3 Microstructure of COCH, COBH and COPH with different mixing ratios.

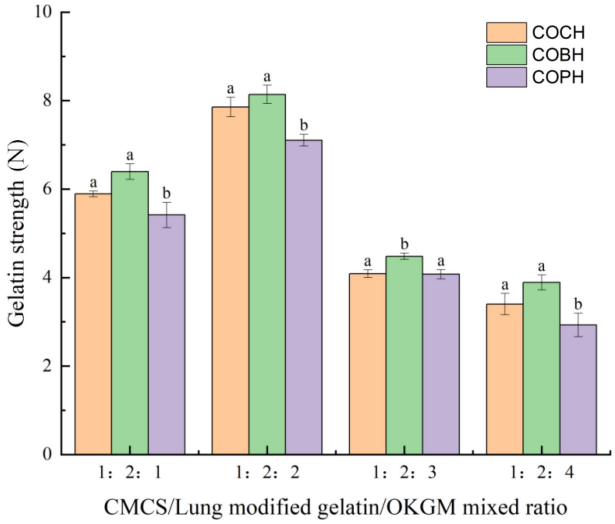

Fig. 4 Gelatin strength of COCH, COBH and COPH with different mixing ratios. The data in this figure is expressed as mean ± SD, different letters in the same material indicates significant differences ($p < 0.05$).

correlation with the study of Xiong[27]. He found that the strength, hardness and adhesion of the composite hydrogel was increased with the increase of polysaccharide. This may be due to the cross-linking of the hydrogel being deepened, leading to an increase in gelatin strength. Schiff base reaction was produced continuously when the ratio of OKGM increased. But the gelatin strength of hydrogel was reduced when OKGM was added with an excessive proportion. It was possible that the hybrid hydrogel might be over-crosslinked to exhibit excessively brittle mechanical properties when the aldehyde group content was too high[28]. Three composite hydrogels of the same mixing ratio were exhibited with different gelatin strengths probably due to their different species origin. Hydrogels usually prepared from high molecular weight gelatin were shown to have high gelatin strength[29].

Swelling ratio

In general, a good food adhesive or coating film can be characterized by the swelling ratio of the hydrogel to its ability to absorb and retain water. As the lyophilized hydrogel was soaked for a longer time, the overall trend of the composite hydrogel swelling was to first increase rapidly and then level off. The results showed that the composite hydrogel had better water absorption and water retention capacity. Composite hydrogels swelled because of hydrophilic groups such as hydroxyl, amino and amide groups in their structure, which allowed the hydrogel to hold a large number of water molecules[30]. As shown in Fig. 5, the swelling rate of composite hydrogels with mixing ratios of 1:2:2, 1:2:1, 1:2:3, and 1:2:4 was gradually decreased, respectively. In general, the high concentration of OKGM was caused the dissolution rate of the composite hydrogel to be reduced. These results were to be expected. This result indicated that increasing the concentration of OKGM allowed the degree of cross-linking to be increased, the pore size to be reduced (as shown in Fig. 5), and the swelling ratio to be reduced[31]. It can be seen that the swelling rate of hydrogel reached the highest level when the mixing ratio of OKGM was 1:2:2. The lowest swelling of the composite hydrogel with a mixing ratio of 1:2:4 might be due to the tightness of its internal structural cross-linked network, which made it difficult for water molecules to enter, and the internal water was firmly locked in the gelatin network. The COBH with the highest swelling ratio had a higher maximum swelling ratio compared to the OKGM/CMCS/graphene oxide hydrogel made by Fan et al.[6] for use as a wound dressing.

Thermal analysis

The thermal stability of various composite hydrogels can be studied by DSC analysis and the results are shown in Fig. 6. The three composite hydrogels had an absorption peak at 60–75 °C at a mixing ratio of 1:2:1. When the mixing ratio of OKGM was increased, the previous absorption peak was disappeared. This result indicated that Schiff base reaction occurs cross-linking was produced (as shown in Fig. 2). The complex and stable network structure was constructed by covalent and non-covalent bonding of polysaccharides and proteins, which increased the denaturation temperature.

As can be seen from Fig. 6, the thermal variation curves of all hydrogel samples showed similar trends. When the temperature ranges from 0 to 120 °C, the reduction of the initial mass of the sample was mainly due to the evaporation of water.[32] Subsequently, mass loss can be attributed to the degradation of exposed OKGM, CMCS and lung-modified gelatin side chains. Polysaccharides were decomposed at high temperatures to produce gaseous products and solid coke.[33] A central peak region appeared near 230 °C. The main reason might be due to the cleavage of physical forces such as electrostatic forces, hydrogen bonds and van der Waals forces in the internal structure of the hydrogel and the imine bonds in the Schiff base reaction. The phenomenon was the same as the results of the collagen-hyaluronic acid *in*

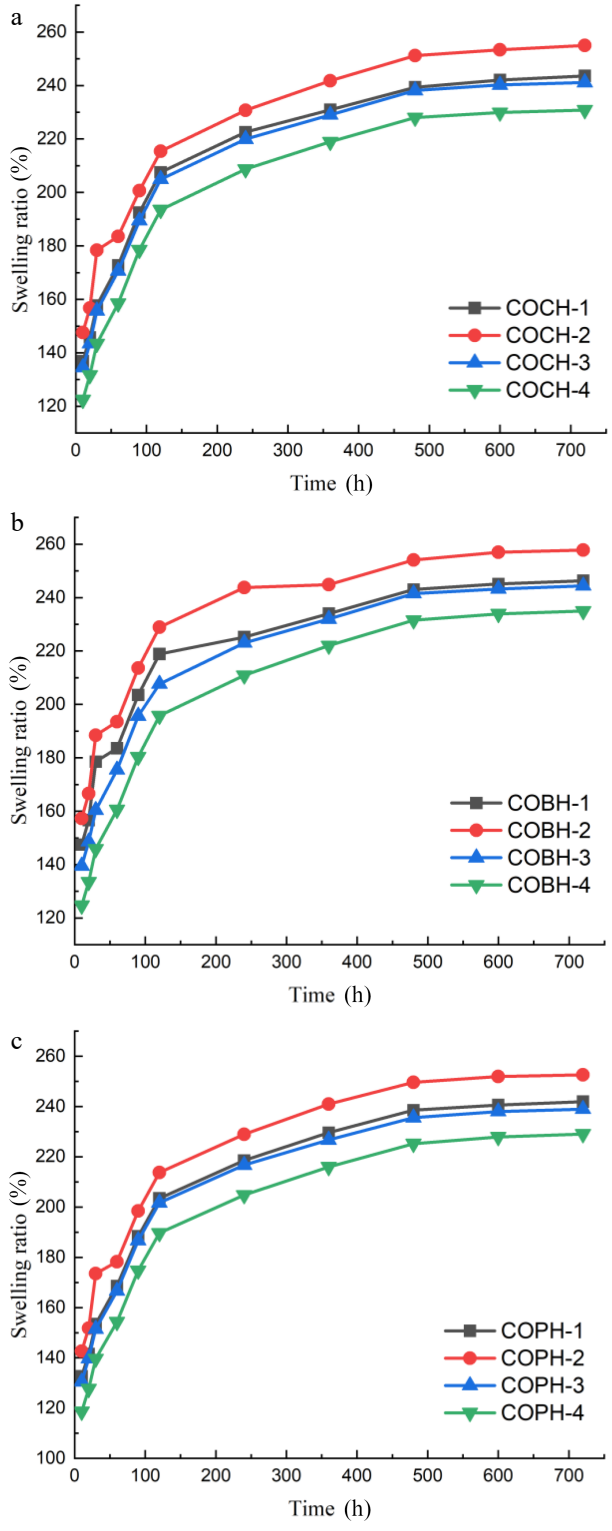

Fig. 5 Swelling rate of (a) COCH, (b) COBH, and (c) COPH with different mixing ratios.

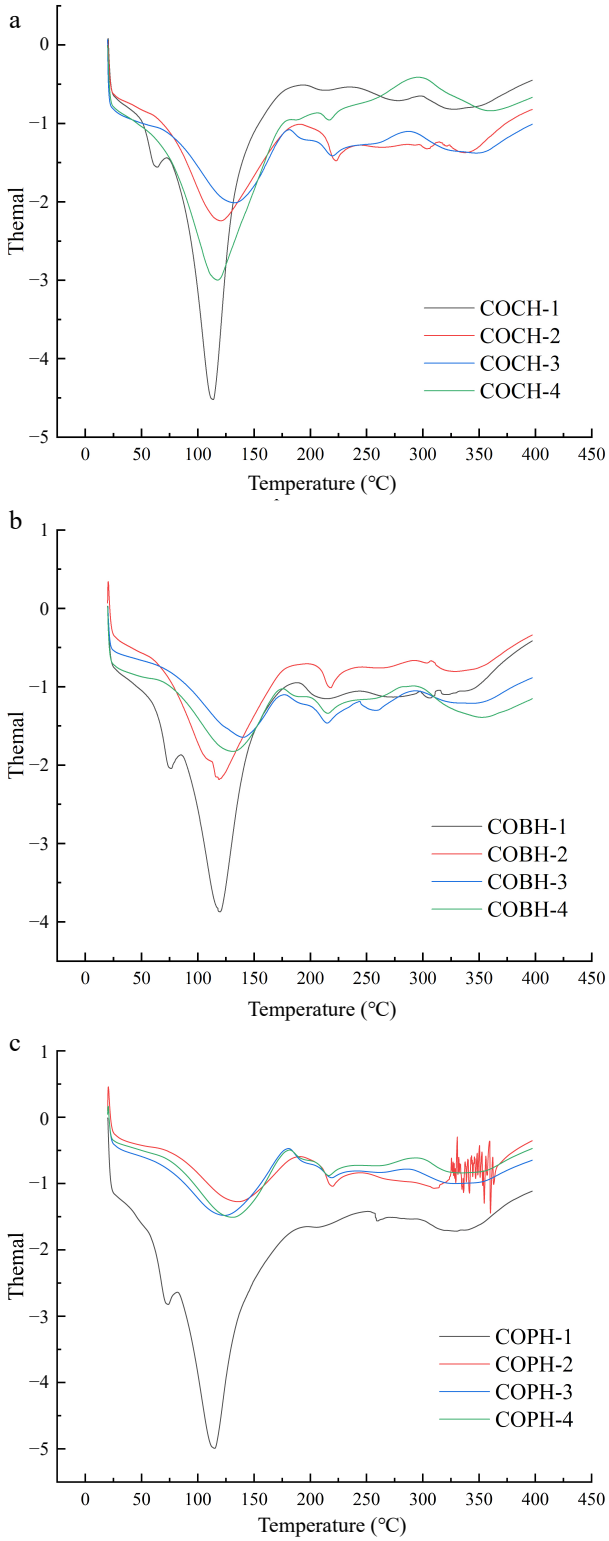

Fig. 6 Thermogravimetric analysis of (a) COCH, (b) COBH, and (c) COPH with different mixing ratios.

situ hydrogel thermal transformation study trend studied by Ying[34]. Further cross-linking of hydrogels led to an increase in thermal denaturation temperature. In this study, the peak areas of the hydrogels prepared with three different mixing ratios and the positions of the peak temperatures corresponding to the regions of the reaction peaks were showed slight deviations. This result suggested that the different strength of interactions within these hydrogels might be related to their different access sources.

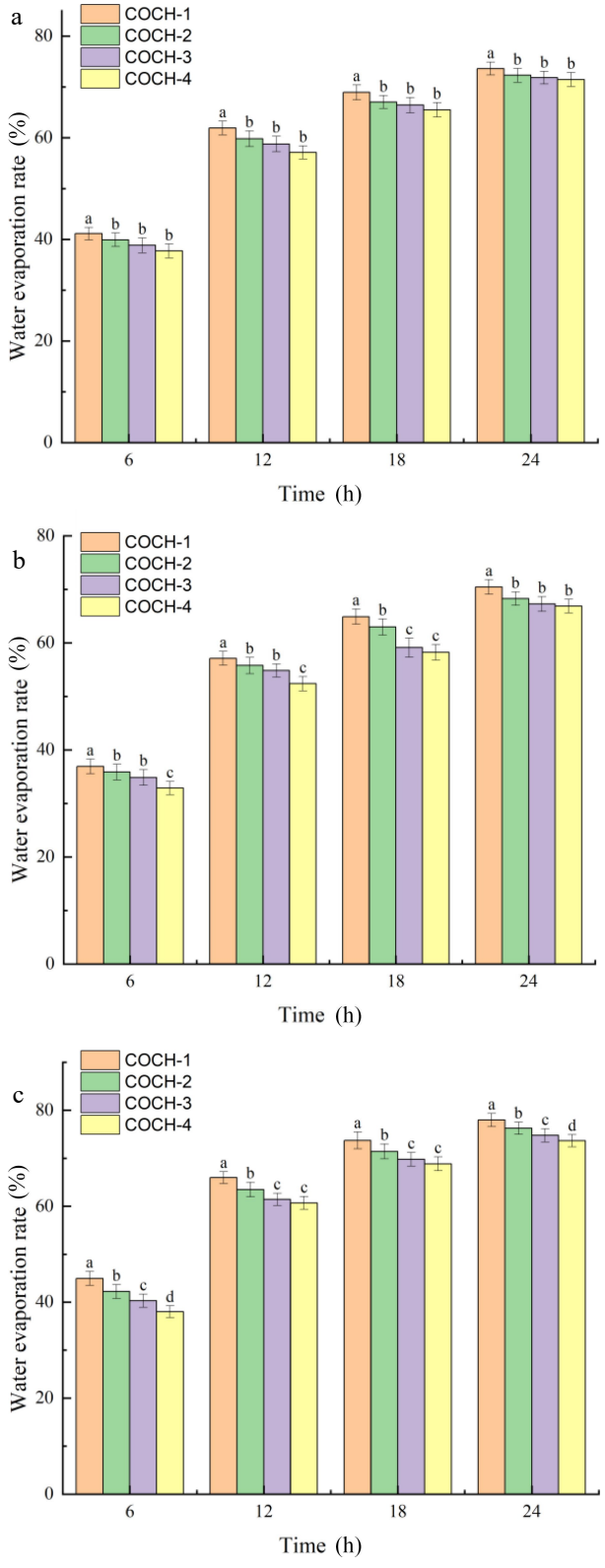

Fig. 7 Moisture evaporation rate of (a) COCH, (b) COBH, and (c) COPH with different mixing ratios.

Water evaporation rate

In general, the moisture content of a food product is very closely related to its food quality. Therefore, the edible and nutritional qualities of foods with lower water evaporation rates can be better preserved. Figure 7 showed the water evaporation rate of hydrogels with different mixing ratios. It can be seen that the water loss rate of all hydrogels was increased rapidly in the first 12 h and then reached a constant percentage in 24 h and maintained 20% to 25% of water content. The results showed that these composite hydrogels all had a low water evaporation rate. The final water evaporation rates of the three composite hydrogels with 1:2:4 mixing ratios in this study were better than the OKGM/CMCS/graphene oxide hydrogels made by Fan et al.[6] The water loss rate of hydrogel was gradually reduced when the OKGM content gradually increases. This might be due to the gradual stabilization of the structure of the gelatin network and the weakening of water mobility within the gelatin structure, as can be seen in Figs 3 & 5. Additionally, the water evaporation rate of three composite hydrogels with the same mixing ratio was the best for COBH and the worst for COPH. It might be related to its gelatin type, and the water holding capacity was affected by the different content of hydrophobic groups in gelatin[35]. This result also affected the water evaporation rate of the composite hydrogel produced.

LF-NMR

The distribution and state of moisture in meat used LF-NMR techniques to analyze the relaxation properties of hydrogen nuclei in samples by measuring them in a magnetic field[36]. The differences in relaxation times and signal magnitudes of T_2 inversion spectra were used to analyze the moisture distribution and migration patterns of COCH, COBH and COPH. As shown in Table 1, the T_2 relaxation inversion spectrum varied from 0.01 to 10,000 ms, and recorded as T_{21} (0.01–10 ms), T_{22} (10–100 ms), and T_{23} (100–1,000 ms) in that order. These three corresponded to bounding water, non-fluidizable water and free water in the composite hydrogel[37]. Binding water (T_{21}) value was the smallest, which was mainly in cell wall fibrous structures, polysaccharide structures, and sieve tube and duct pores[38]. Non-fluidizable water (T_{22}) value was the next best, which was mainly in the cytoplasm in the form of enzymes, hydrated hemisaccharides, intermediate metabolites, and macromolecules. The free water (T_{23}) value was the largest and it existed mainly in free form in the vesicles. Additionally, the T_2 peak area in the spectrum was proportional to the number of hydrogen protons in the sample[39]. Therefore, the content of water in the three states of bounding water, non-fluidizable water and free water were represented by P_{21}, P_{22} and P_{23}.

As shown in Table 1, with the constant addition ratio of CMCS and modified gelatin, P_{21} and P_{22} of COCH, COBH and COPH showed an increasing trend and P_{23} showed a decreasing trend with the increasing addition of OKGM. This indicated that the conversion of free water to non-fluidizable water and bounding water in the hydrogel was gradually enhanced as the ratio of OKGM increased, resulting in an increase in water retention capacity. This reason might be due to the generation of Schiff base reaction. The internal network structure of hydrogel became more dense. The free water was converted into non-fluidizable water, and the stability was greatly enhanced. Additionally, the value of homogeneous hydrogel T_{23} gradually decreased with the increase of OKGM addition. This result was similar to the

Table 1. Low-field nuclear magnetic characterization of COCH, COBH and COPH with different mixing ratios.

	T_{21} (ms)	T_{22} (ms)	T_{23} (ms)	P_{21}	P_{22}	P_{23}
COCH-1	3.152 ± 0.437^{a}	27.466 ± 0.953^{a}	530.627 ± 0.100^{e}	24.990 ± 0.394^{d}	7649.545 ± 0.963^{m}	173.803 ± 3.172^{d}
COCH-2	2.676 ± 0.487^{a}	19.902 ± 0.468^{c}	526.32 ± 0.798^{e}	$27.593 \pm 0.585^{c,d}$	7914.01 ± 1.024^{h}	166.833 ± 2.574^{e}
COCH-3	$1.978 \pm 0.633^{a,b}$	$17.544 \pm 0.200^{c,d}$	581.293 ± 1.175^{d}	30.025 ± 0.370^{c}	7972.7 ± 1.590^{e}	167.659 ± 0.626^{e}
COCH-4	0.675 ± 0.088^{c}	14.759 ± 0.058^{d}	332.846 ± 0.881^{h}	$32.866 \pm 0.355^{a,b}$	8506.39 ± 3.585^{b}	153.705 ± 1.037^{g}
COCH-1	2.7845 ± 0.731^{a}	23.558 ± 1.133^{b}	581.118 ± 1.000^{d}	35.838 ± 1.079^{a}	7775.183 ± 2.558^{l}	178.562 ± 1.297^{d}
COCH-2	2.401 ± 1.091^{a}	$17.012 \pm 1.604^{c,d}$	483.093 ± 1.696^{g}	30.917 ± 0.319^{c}	7944.58 ± 3.422^{g}	161.966 ± 0.922^{f}
COCH-3	$1.5705 \pm 0.484^{a,b}$	$17.6185 \pm 1.017^{c,d}$	504.607 ± 0.050^{f}	33.752 ± 1.111^{a}	8295.7 ± 0.714^{d}	153.496 ± 2.485^{g}
COCH-4	0.557 ± 0.086^{c}	13.601 ± 0.200^{d}	303.613 ± 0.945^{i}	33.392 ± 0.177^{a}	8912.46 ± 2.481^{a}	124.857 ± 0.607^{h}
COPH-1	3.382 ± 0.260^{a}	26.308 ± 0.714^{a}	719.183 ± 1.966^{b}	$26.274 \pm 3.302^{c,d}$	7403.543 ± 0.526^{n}	256.824 ± 0.806^{a}
COPH-2	2.675 ± 1.422^{a}	19.635 ± 0.999^{c}	627.106 ± 0.112^{c}	$28.1985 \pm 0.773^{c,d}$	7857.69 ± 1.734^{i}	216.393 ± 0.314^{b}
COPH-3	2.072 ± 1.050^{a}	$17.586 \pm 0.048^{c,d}$	765.049 ± 1.832^{a}	31.524 ± 0.061^{b}	7952.09 ± 1.003^{f}	193.956 ± 1.258^{c}
COPH-4	1.548 ± 0.108^{b}	$16.209 \pm 1.508^{c,d}$	506.198 ± 1.641^{f}	31.542 ± 0.182^{b}	8331.59 ± 0.7845^{c}	176.078 ± 2.867^{d}

The data in this table is expressed as mean ± SD, different letters in the same column indicates significant differences ($p < 0.05$).

previous study by Chitrakar et al.[40], who suggested that the mobility of water was decreased with the addition of polysaccharides due to the binding between polysaccharide molecules. As the concentration of polysaccharides increased, tighter linkages between polysaccharide molecules occurred, depending mainly on the molar mass of the polysaccharide and inter-chain interactions[41]. At the same time, water molecules were slower to reorient in denser network structures because they were more tightly bound to biopolymers with hydrogen bonds[42]. The decrease in T_{23} value was due to that more water molecules were locked in the polysaccharide structure resulting in a gradual decrease in mobility as the polysaccharide concentration increases.

Antibacterial properties

Hydrogels with antibacterial properties have a wide range of potential applications in the food industry. Figure 8 represents the inhibition of *E. coli* and *S. aureus* by composite hydrogels at different mixing ratios. The results showed that all composite hydrogels exhibited inhibitory effects on both *E. coli* and *S. aureus*. The best antibacterial effect of composite hydrogel was COBH hydrogel. When the hydrogel mixing ratio was 1:2:2, the antibacterial effect of *E.coli* was 38.02%, and the antibacterial effect of *S.aureus* was 37.39%. Because more CMCS can cross-link with OKGM to form a hydrogel with a network structure and thus the antibacterial activity was enhanced when the OKGM content increased. This result was consistent with the finding of Bozaci et al.[43] When the CMCS content in hydrogel films was 6%, the corresponding films exhibited desirable antimicrobial properties. CMCS had an inhibitory effect on bacteria by changing the permeability of the bacterial cell wall through the interaction of its cations with the anionic groups of the bacterial cell wall.[44] However, as the OKGM content continued to increase, the antibacterial activity of the hydrogel was slightly weakened instead of enhanced. This appearance was due to the fact that the gelatin structure became denser in structure, the pore size became smaller, and the carboxymethyl group was difficult to contact with bacteria. These composite hydrogels of COBH and COCH can be used in food packaging and preservation.

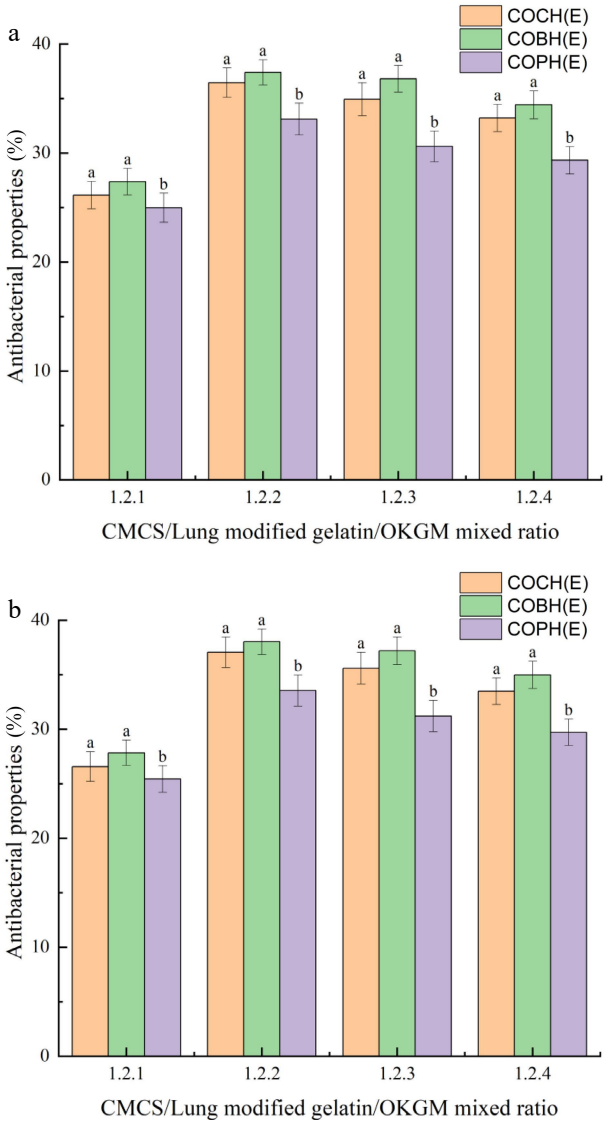

Fig. 8 (a) Anti-*S. aureus* and (b) *E. coli* activity of COCH, COBH and COPH with different mixing ratios.

Conclusions

In this paper, the swelling rate, gelatin strength, and antibacterial properties of composite hydrogel increased initially and then decreased with the increase of OKGM ratio. The best swelling performance, gel strength and the

strongest inhibition of *E. coli* and *S. aureus* was observed when lung gelatin/CMCS/OKGM was added in the ratio of 1:2:2 for COCH, COBH and COPH, respectively. The water evaporation rate of composite hydrogels all gradually decreased with the increase of OKGM ratio. The lowest water evaporation rate was achieved when the lung gelatin/CMCS/OKM addition ratio was 1:2:4. Interestingly, the hydrogel properties of COCH and COBH were interchangeable, but all were significantly different from COPH. Therefore, COCH have potential applications in food coating and preservation.

Author contributions

The authors confirm contribution to the paper as follows: methodology: Zou Y, Lan Y, Qin X, and Wang Z; validation & formal analysis : Zou Y; resources: Wang D; investigation: Zou Y, Wang X, Liang Li, Wang L, Lan Y, Qin X, Wang Z, and Wang D; draf manuscript: Zou Y, Wang X, Liang Li, and Wang L; review & editing manuscript: Wang X, Liang Li, and Wang L; project administration: Xu W. All authors reviewed the results and approved the final version of the manuscript.

Data availability

All data generated or analyzed during this study are included in this published article.

Acknowledgments

This work was supported by the China Agriculture Research System (CARS-41) and Key Research, Jiangsu Agriculture Science and Technology Innovation Fund (CX (21)2016) and Liaocheng Science and Technology Support SME Climbing Plan Project (2023PDJH23).

Conflict of interest

The authors declare that they have no conflict of interest.

Dates

Received 15 August 2023; Accepted 17 October 2023; Published online 5 December 2023

References

1. Naahidi S, Jafari M, Logan M, Wang Y, Yuan Y, et al. 2017. Biocompatibility of hydrogel-based scaffolds for tissue engineering applications. *Biotechnology Advances* 35(5):530–44
2. Liang Y, Zhao X, Ma PX, Guo B, Du Y, et al. 2018. pH-responsive injectable hydrogels with mucosal adhesiveness based on chitosan-grafted-dihydrocaffeic acid and oxidized pullulan for localized drug delivery. *Journal of Colloid and Interface Science* 536:224–34
3. Poverenov E, Zaitsev Y, Arnon H, Granit R, Alkalai-Tuvia S, et al. 2014. Effects of a composite chitosan-gelatin edible coating on postharvest quality and storability of red bell peppers. *Postharvest Biology and Technology* 96:106–09
4. Bai H, Li Z, Zhang S, Wang W, Dong W. 2018. Interpenetrating polymer networks in polyvinyl alcohol/cellulose nanocrystals hydrogels to develop absorbent materials. *Carbohydrate Polymers* 200:468–76
5. Ge S, Liu Q, Li M, Liu J, Lu H, et al. 2018. Enhanced mechanical properties and gelling ability of gelatin hydrogels reinforced with chitin whiskers. *Food Hydrocolloids* 75:1–12
6. Fan L, Yi J, Tong J, Zhou X, Ge H, et al. 2016. Preparation and characterization of oxidized konjac glucomannan/carboxymethyl chitosan/graphene oxide hydrogel. *International Journal of Biological Macromolecules* 91:358–67
7. Cao L, Chen C, Zhou Z, Dou S, Yun S, et al. 2022. Preparation of carboxymethyl chitosan/oxidized carboxymethyl cellulose/curcumin composite film and its application in strawberry film coating for preservation. *Modern Food Technology* 38(12):247–54
8. Cai M, Xie Y, Zhou Y, Zhang S, Li Y, et al. 2022. Effect of konjac glucomannan on the properties of β-glucan complex gels. *Food and Fermentation Industries* 48(16):223–29
9. Han Q, Zhou T, Li Y, Li G, Song Z, et al. 2023. Effects on starch properties and application in functional foods of konjac glucomannan. *Food Industry Technology* 44:441–47
10. Jiang Y, Li G, Wang H, Li Q, Tang K. 2022. Multi-crosslinked hydrogels with instant self-healing and tissue adhesive properties for biomedical applications. *Macromolecular Bioscience* 22:e2100443
11. Yan J. 2018. *Preparation and evaluation of the properties of asparagus pollen polysaccharide/astragalus polysaccharide hydrogel*. Thesis. Lanzhou University of Technology, China.
12. Shi P, Liu M, Fan F, Yu C, Lu W, et al. 2018. Characterization of natural hydroxyapatite originated from fish bone and its biocompatibility with osteoblasts. *Materials Science & Engineering: C* 90:706–12
13. Fan M, Hu T, Zhao S, Xiong S, Xie J, et al. 2017. Gel characteristics and microstructure of fish myofibrillar protein/cassava starch composites. *Food Chemistry* 218:221–30
14. Fan L, Yang H, Yang J, Peng M, Hu J. 2016. Preparation and characterization of chitosan/gelatin/PVA hydrogel for wound dressings. *Carbohydrate Polymers* 146:427–34
15. Liu L, Wen H, Rao Z, Zhu C, Liu M, et al. 2018. Preparation and characterization of chitosan–collagen peptide/oxidized konjac glucomannan hydrogel. *International Journal of Biological Macromolecules* 108:376–82
16. Jiang S. 2022. *Strength and anisotropy regulation of konjac glucomannan/xanthan gum/sodium alginate composite gels*. Thesis. Huazhong Agricultural University, China.
17. Bian S, Zheng Z, Liu Y, Ruan C, Pan H, et al. 2019. A shear-thinning adhesive hydrogel reinforced by photo-initiated crosslinking as a fit-to-shape tissue sealant. *Journal of Materials Chemistry B* 7:6488–99
18. Huang C, Zhu D, Jiang T, Xu J. 2022. Preparation and properties of PVA/CMCS /OCD hydrogel for artificial blood vessels. *Modern Chemical* 42:152–159+165
19. Wang B, Liu S, Fan I, Chen T, Sun H, et al. 2022. Preparation and properties of carboxybutyryl chitosan-silk peptide/oxidized konjac injectable hydrogel. *Journal of Wuhan University (Science Edition)* 68(6):589–92
20. Sun Y, Luo A, Feng J, Lu J, Liu Q, et al. 2019. Preparation and properties of oxidized konjac glucomannan-chitosan composite films. *Food and Fermentation Industry* 45(5):170–76
21. Tian W, Qin X, Xie Y, Chen C, Long M, et al. 2022. Preparation and properties of oxidized konjac glucomannan-chitosan composite films. *Food and Fermentation Industry* 00:1–10
22. Kasahara H, Tanaka E, Fukuyama N, Sato E, Sakamoto H, et al. 2003. Biodegradable gelatin hydrogel potentiates the angiogenic effect of fibroblast growth factor 4 plasmid in rabbit hindlimb ischemia. *Journal of the American College of Cardiology* 41:1056–62
23. Sun J, Jiang H, Wu H, Tong C, Pang J, et al. 2020. Multifunctional bionanocomposite films based on konjac glucomannan/chitosan with nano-ZnO and mulberry anthocyanin extract for active food packaging. *Food Hydrocolloids* 107:105942

24. Wu H, Wu H, Qing Y, Wu C, Pang J. 2022. KGM/chitosan bionanocomposite films reinforced with ZNPs: Colloidal, physical, mechanical and structural attributes. *Food Packaging and Shelf Life* 33:100870
25. Liu J, Wang Z, Jiang X, Cao Y. 2018. Gelatin-chitosan-sodium alginate gel-embedded papain. *Food Industry Technology* 39:1–5
26. Luo M, Zhuo Y, Yang Y, Shan W. 2013. Preparation and performance study of a novel gel system for traumatic surfaces. *China Journal of Pharmaceutical Industry* 44:1232–35
27. Xiong Z. 2010. Characterization of gel texture of soybean isolate protein-anion polysaccharide composite system. *Grain and Oil Processing* 2010:133–36
28. Li G. 2021. *Study of gelatin-based antibacterial adhesive composite hydrogels*. Thesis. Zhengzhou University, China.
29. Nagarajan M, Benjakul S, Prodpran T, Songtipya P, Kishimura H. 2012. Characteristics and functional properties of gelatin from splendid squid (*Loligo formosana*) skin as affected by extraction temperatures. *Food Hydrocolloids* 29:389–97
30. Liu K. 2019. *Development of chitosan hydrogel and its modification*. Thesis. Wuhan University of Technology, China.
31. Wang M, Gu J, Hao Y, Qin X, Yu Y, et al. 2023. Adhesive, sustained-release, antibacterial, cytocompatible hydrogel-based nanofiber membrane assembled from polysaccharide hydrogels and functionalized nanofibers. *Cellulose* 30:323–37
32. Guo Y, Huang W, Mao X. 2022. Preparation and Release Properties of pH Responsive Carboxymethyl Agarose-Polydopamine Hydrogel. *Food Science* 43(10):59–65
33. Chen X, Pang J, Wu C. 2021. Fabrication and characterization of antimicrobial food packaging materials composed of konjac glucomannan, chitosan and fulvic acid. *Food Science* 42(7):232–39
34. Ying H. 2019. *Research on collagen-glycosaminoglycan based biomaterials and their application in tissue engineering*. Thesis. Jiangnan University, China.
35. Kwak HW, Shin M, Lee JY, Yun H, Song DW, et al. 2017. Fabrication of an ultrafine fish gelatin nanofibrous web from an aqueous solution by electrospinning. *International Journal of Biological Macromolecules* 102:1092–103
36. Fan D, Ma S, Wang L, Zhao H, Zhao J, et al. 2013. ^{1}H NMR studies of starch–water interactions during microwave heating. *Carbohydrate Polymers* 97:406–12
37. Cheng S, Wang X, Li R, Yang H, Wang H, et al. 2019. Influence of multiple freeze-thaw cycles on quality characteristics of beef *semimembranous* muscle: With emphasis on water status and distribution by LF-NMR and MRI. *Meat Science* 147:44–52
38. Lahaye M, Falourd X, Laillet B, Le Gall S. 2020. Cellulose, pectin and water in cell walls determine apple flesh viscoelastic mechanical properties. *Carbohydrate Polymers* 232:115768
39. Yue X, Bai Y, Wang Z, Song P. 2020. Low-field nuclear magnetic resonance study of maize seed germination process under salt stress. *Journal of Agricultural Engineering* 36(24):292–300
40. Chitrakar B, Zhang M, Bhandari B. 2019. Novel intelligent detection of safer water activity by LF-NMR spectra for selected fruits and vegetables during drying. *Food and Bioprocess Technology* 12(7):1093–101
41. Duxenneuner MR, Fischer P, Windhab EJ, Cooper-White JJ. 2008. Extensional properties of hydroxypropyl ether guar gum solutions. *Biomacromolecules* 9:2989–96
42. Alvarez MD, FerncLndez C, Canet W. 2009. Enhancement of freezing stability in mashed potatoes by the incorporation of kappa-carrageenan and xanthan gum blends. *Journal of the Science of Food and Agriculture* 89:2115–27
43. Bozaci E, Akar E, Ozdogan E, Demir A, Altinisik A, et al. 2015. Application of carboxymethylcellulose hydrogel based silver nanocomposites on cotton fabrics for antibacterial property. *Carbohydrate Polymers* 134:128–35
44. Wang YL, Zhou YN, Li XY, Huang J, Wahid F, et al. 2020. Continuous production of antibacterial carboxymethyl chitosan-zinc supramolecular hydrogel fiber using a double-syringe injection device. *International Journal of Biological Macromolecules* 156:252–61